# Analysis of Network Structure of UV-Cured Acrylates by $^1$H NMR Relaxation, $^{13}$C NMR Spectroscopy, and Dynamic Mechanical Experiments

**V. M. Litvinov* and A. A. Dias**

*DSM Research, P.O.Box 18, 6160 MD Geleen, The Netherlands*

*Received January 16, 2001*

ABSTRACT: The network structure of UV-cured acrylates was analyzed by dynamic mechanical experiments, $^1$H $T_2$ NMR relaxation, and $^{13}$C NMR spectroscopy. Photocured mixtures of difunctional (poly(ethylene glycol) diacrylate) and monofunctional (2-ethylhexyl acrylate) were studied. The mean cross-link density and fraction of dangling chains were varied in these networks by changing the content of monofunctional acrylate. Examining networks by $^{13}$C NMR spectroscopy, we observed that the conversion is high, and the contribution or the effect of side reactions that generate extra cross-links is negligible. The spatial distribution of cross-links is very heterogeneous in the cured samples; i.e., polyacrylate ziplike network junctions are interconnected by polyether chains. An increase in the content of monofunctional monomer causes a significant decrease in the cross-link density because the monofunctional monomer acts as a chain extender. NMR $T_2$ relaxation method shows good correlation with mechanical tests with respect to molar mass between cross-links, $M_c$. Obtained values of $M_c$ are significantly smaller compared to molar mass of diacrylate. As anticipated, it is apparent that classical rubber elasticity theories are not applicable for characterization of this type of networks containing ziplike network junctions.

## Introduction

Several curing procedures are used to prepare cross-linked polymers. Among these procedures, photocuring offers several advantages, including cure speed, reduced emission (solvent free), and ease of applicability. UV curing has found an increased use in not only coatings but also adhesives, dental curing resins and photofabrication of 3-D objects—stereolithography. With the increasing importance of the radiation cure much effort is devoted to fabrication of coatings or objects of specified mechanical properties.

Mechanical and elastic properties of unfilled, cross-linked elastomers are largely influenced by the mean molar mass of viscoelastic chains between chemical and physical network junctions, type of network junctions, and network imperfections and heterogeneity. To relate mechanical properties to chemistry, it is essential to understand the network topology of the resultant cured materials. Despite apparent simplicity, the network structure has complex topology, which can significantly affect functional properties. Different types of network heterogeneities are present in the cured material, if no special precautions are taken to control curing chemistry and conditions. A difference in curing conditions through the sample volume, such as UV dose and temperature, results in *spatial heterogeneity* of the network structure. The type of photoinitiators as well as chemical composition of oligomer chains could cause *molecular scale heterogeneity* of the network. The following heterogeneous structures can be present: heterogeneity in distribution of network junctions, unattached to network chains, dangling chains, and loops. Furthermore, the mechanical properties can also be affected by[1] the type of network junctions [i.e., functionality and bulkiness that determines ability of network junctions to fluctuate (affine vs phantom networks)],[2] chain entanglements,[3] small crystallinity,[4] and specific interactions between polymer chains caused by for example hydrogen bonds and microphase separation. These variables can be utilized to modify properties of cured materials. However, they also cause difficulties in reliable analysis of the network structure and complicate the effort to establishing structure−property relationships.

Generally, methods that are used for analysis of network structure can be subdivided into three categories based on the methodology:

*1. Characterization of physical properties of cured materials* in relation to volume-average network density. The most common methods are equilibrium swelling and mechanical measurements.[1,2] In addition to the network structure, these methods provide information that is desirable for practical applications, such as modulus, stress−strain behavior, and glass transition temperature. Rubber elasticity theory and phenomenological theories are used to relate a measured quantity to the density of chemical and physical cross-links. Several molecular models have been developed for "ideal" networks in which no defects are present.[2−5] However, there is a considerable debate about the validity and applicability of these models, and several discrepancies between theory and experiment still remain, e.g., the role of chain entanglements, network defects, and network heterogeneity. It is acknowledged that traditional methods are not capable of providing complete reliable information about network topology.[5−7]

*2. Analysis of chemical conversion and cure chemistry* is another way to study the network structure. Several techniques are used for this purpose, e.g., optical spectroscopy,[8] high-resolution NMR spectroscopy, and titration of nonreacted functional groups. The spectroscopic methods can be used for quantitative analysis of cross-links.[9−11] Chemical conversion is usually closely related to the network density. However, no exact quantitative information on the network structure can be obtained, since reacted groups can form not only

* To whom correspondence should be addressed.

10.1021/ma010066u CCC: $20.00 
Published on Web 05/11/2001

chemical cross-links but also viscoelastically ineffective chains, such as chain branches and chain loops. Furthermore, side reactions, which easily can cause additional cross-links, complicate data interpretation due to overlapping of signals from different types of chemical groups in complex mixtures. Moreover, physical network junctions are hardly detected by spectroscopic methods.

*3. Analysis of molecular mobility of polymer chains* is used to study the network density and its heterogeneity. Dynamic mechanical analysis and dielectric spectroscopy provide information about mobility of polymer chains, which is linked to the network density. One of the most informative and sensitive methods is solid-state NMR.[12−14] NMR imaging or microscopy is used for determination of spatial heterogeneity of rubbery materials on the scale of 15−50 $\mu$m.[14−16] Different types of NMR relaxation experiments are used for analysis of local and long-range spatial mobility of polymer chains. Since chain motion is strongly coupled to the length of network chains, chemical information on network structure and network defects can be obtained in this way. Selective information on the mobility of polymer chain units of different chemical origin can be obtained by means of selective NMR relaxation experiments. Relationships between NMR relaxation parameters and dielectric and mechanical properties have been established.[17−19]

Apparently, the most comprehensive information on the network structure in the relation to properties can be obtained by these three complementary methodologies.

A number of NMR methods were applied to study kinetics of radical curing and the structure of resultant networks. $^1$H and $^{13}$C NMR spectroscopies have been used for monitoring the conversion of various acrylates.[20−26] Differences in reactivity between various double bonds in a cross-linking system were also determined in these studies. $^{13}$C NMR $T_1$ and $T_{1\rho}(^1\text{H})$ experiment were used to make the distinction between constrained and unconstrained local surroundings and to relate these differences to chemical origin of network heterogeneity. The growth of cross-linked clusters and partial phase separation due to difference in the monomer reactivity were suggested by these studies. This interpretation was supported by spin-diffusion experiments, which reveal nanometer scale heterogeneity of networks.[20,21] Different authors demonstrated good agreement in chemical conversion as measured with NMR and optical spectroscopy[20,21] and reaction enthalpies as described by Moore.[27] $^1$H and $^{13}$C NMR spectroscopies can also be used to monitor real time UV-curing of acrylates.[28] It was shown in this study that chemical conversion against curing time could be well described by a theory, which takes into account a difference in reactivity of acrylates in mixtures.

Analysis of chain mobility with respect to cross-link density using NMR relaxation experiments has been reviewed by several authors.[29−32] NMR relaxation times $T_1$ and $T_{1\rho}$ are largely affected by local segmental mobility on the order of 100 MHz and 50 kHz, respectively. Curing causes a decrease in local chain mobility, as was shown by several authors.[22−26] A linear dependence of $1/T_1$ on the inverse of the molecular weight of network chains is observed to be similar to that of the glass temperature.[33] It is recognized that a moderate change in $T_1$ and $T_{1\rho}$ relaxation times is observed for networks with low cross-link density. This limits applicability of these relaxation experiments for quantitative analysis of network density. On the other hand, $T_2$ relaxation is very sensitive to even small differences in the cross-link density, because this relaxation time for rubbery materials is largely governed by constraints on large spatial-scale chain mobility imposed by chemical and physical cross-links.[31] Since chain motion is strongly coupled to elastomer structure, chemical information can be obtained in this way. A comparison of the cross-link density, as measured by $T_2$ relaxation experiments, with that obtained by traditional methods for the same samples proves that the NMR method provides quantitative data on the cross-link density.[11,33,34] Therefore, $T_2$ relaxation is preferred over $T_1$ and $T_{1\rho}$ relaxations as a probe for network structure.

In addition to the mean cross-link density, the analysis of $T_2$ relaxation can provide information on network defects and heterogeneous distribution of network junctions. The sensitivity of the $T_2$ experiments to the molecular scale heterogeneity is due to the local origin of the relaxation process, which is predominantly governed by the near-neighbor environment and intrachain effects for $T_2$ relaxation at temperatures well above the $T_g$. Therefore, the submolecules concept can be used to describe the relaxation behavior.[31] In a simplified picture, the total $T_2$ relaxation decay for a heterogeneous elastomer is a weighted sum of decays from the different submolecules which are defined as network chains between the chemical and the physical junctions, chain loops, and chain-end blocks. These submolecules possess different relaxation behavior due to differences in the large spatial scale mobility. The relative contribution of the submolecules to the total proton $T_2$ relaxation decay is proportional to the number of protons, which are attached to these chain fragments. A quantitative analysis of the decay shape is not always straightforward due to the complex origin of the relaxation function itself[31] and the structural heterogeneity of the long chain molecules. Nevertheless, several examples of the detection of structural heterogeneity by $T_2$ experiments have been published, for example, the analysis of the gel/sol content in cured[35,36] and filled elastomers,[37,38] the estimation of the fraction of chain-end blocks in linear and network elastomers,[39−41] and the determination of a distribution function for the molecular mass of network chains in cross-linked elastomers.[42,43]

The advantage of NMR relaxation experiments is that with minimal sample preparation selective determination of the network structure in rubbery phases in complex materials is possible. Network structure of UV-cured acrylates is analyzed in the present study by mechanical experiments, $T_2$ NMR relaxation, and $^{13}$C NMR spectroscopy. Mixtures of a di- and monofunctional acrylate are used as a model system for this study. The di- and monofunctional acrylates are poly(ethylene glycol) diacrylate (PEGDA) and 2-ethylhexyl acrylate (EHA), respectively. The mean cross-link density and the fraction of network defects are varied in these networks by changing the content of monofunctional acrylate. The aim of the present study is (1) to determine possible side reactions (2), to find a relation between the mechanical properties, as measured by DMA, and the network structure, as probed by NMR $T_2$ relaxation experiments, and (3) to reveal the effect of ziplike network junctions on mechanical properties of cured acrylates.

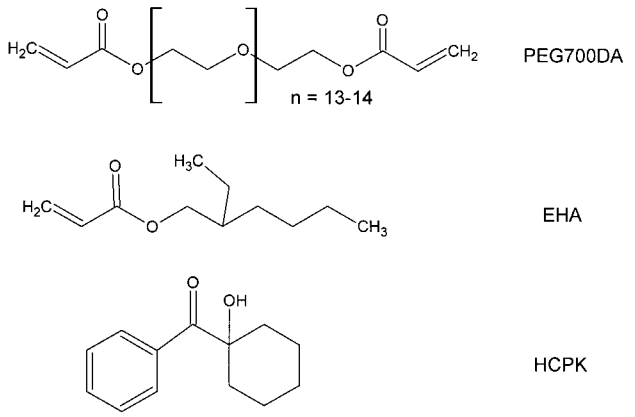


**Figure 1.** Chemical structures of initial compounds.

**Table 1. Sample Composition**

| sample | PEGDA (in mass %) | EHA (in mass %) | PEGDA:EHA (molar ratio) |
|---|---|---|---|
| 1 | 100 | 0 | 1:0 |
| 2 | 90 | 10 | 1:0.2 |
| 3 | 80 | 20 | 1:1 |
| 4 | 70 | 30 | 1:1.2 |
| 5 | 60 | 40 | 1:2.2 |
| 6 | 50 | 50 | 1:4.1 |
| 7 | 40 | 60 | 1:6.2 |
| 8 | 30 | 70 | 1:9.7 |
| 9 | 20 | 80 | 1:16.6 |
| 10 | 10 | 90 | 1:37.5 |

## Experimental Section

**A. Initial Chemicals.** The model system were composed of mixtures of a poly(ethylene glycol) diacrylate (PEGDA) with $M_n = 700$ g/mol and a monofunctional 2-ethylhexyl acrylate (EHA) (Figure 1). The mixtures contained 1 mass % of photoinitiator 1-hydroxycyclohexyl phenyl ketone (HCPK). The specific density of PEGDA and EHA is 1.11 and 0.885 g/cm$^3$, respectively. PEGDA and EHA were obtained from Aldrich Chemical Co. HCPK (Irgacure 184) was supplied by Ciba Geigy.

**B. Sample Composition and Photocuring.** The weight fraction of EHA was varied from 0 to 90% (see Table 1). The mixtures are designated with numbers [i.e., PEGDA/EHA(70:30)], which represents the content of the difunctional monomer in mass percent. Films of 0.1 mm thickness were cured on glass plates at 27 °C on a conveyor belt fitted with a Fusion F600 (6000 W) electrodeless H bulb and with nitrogen inerting. An UV dose of 1 J/cm$^2$ was determined using an UV Power Puck light meter. The chemical conversion was determined by ATR-FT-IR by measuring the peak intensity of acrylate (C−H deformation) at 810 cm$^{-1}$.[44] It was shown that the conversion of acrylate double bonds on both sides of the films (substrate and top) was above 96%. The specific density of the mixtures was calculated on the basis of the densities of PEGDA and EHA, 1.11 and 0.885 g/cm$^3$, respectively. A decrease in sample volume due to shrinkage and thus density increase was neglected in this calculation.

**C. Mechanical Testing.** The glass temperature and the storage modulus were measured with a Rheometrics solid analyzer II (RSA-II) at a frequency of 1 Hz. Test bar samples of 2 mm width and 40 mm length were cut out of the cured films on glass plates and detached from the glass. The thickness of test bars was measured with a calibrated Heidenhain measuring device. The dynamic mechanical tests were performed using the ASTM norm D5026 on RSA-II. The measurements of the storage modulus ($E'$), the loss modulus ($E''$), and the tangent delta were carried out at a frequency of 1 Hz. Experiments were started at −130 °C and the temperature raised to 200 °C with a ramp speed of 5 °C/min.

**D. $^{13}$C NMR Spectroscopy.** $^{13}$C MAS and CP/MAS NMR spectra were recorded on a Varian Inova 400 MHz wide bore NMR spectrometer operating at $^{13}$C frequency of 100.58 MHz, using a 7 mm CP/MAS probe. The $^1$H and $^{13}$C 90° pulse width was about 5 $\mu$s. All experiments were carried out with magic-angle spinning, using a spinning frequency of 2 kHz and high-power proton decoupling. Adamantane was used to optimize the Hartmann−Hahn condition. $^{13}$C chemical shifts were referenced to the methylene resonance of adamantane (38.3 ppm relative to tetramethylsilane). The recycling delay time of 100 and 5 s was used to record $^{13}$C MAS and $^{13}$C CP/MAS spectra, respectively. The number of transients used was 4000 and 17 000 for $^{13}$C MAS and CP/MAS spectra, respectively. To enhance the spectra resolution for cured compounds, the spectra were recorded on samples that had been swollen in $CHCl_3$. The $^{13}$C resonance of $CHCl_3$ does not overlap with peaks of interest. The predicted value of chemical shifts was calculated with a program ACD/CNMR Predictor 4.0.

**E. $^1$H NMR $T_2$ Relaxation Experiment.** The proton transverse magnetization decays, $T_2$ relaxation decays, were measured on a Bruker Minispec NMS-120 spectrometer at a proton resonance frequency of 20 MHz. This spectrometer was equipped with a BVT-3000 variable temperature unit. The temperature gradient and stability were about 1 K and 0.1 K, respectively.

The decay of the transverse magnetization was measured with the Hahn-echo pulse sequence (HEPS), $90°_x - t_{He} - 180°_x - t_{He}$−(acquisition), where $t_{He} \geq 35$ $\mu$s. An echo signal is formed after the second pulse in the HEPS with a maximum at time $t = 2t_{He}$ after the first pulse. By varying the pulse spacing in the HEPS, the amplitude of the transverse magnetization, $A(t)$, is measured as a function of time $t$.

The $T_2$ relaxation experiments were performed on samples as whole and swollen samples. A certain amount of 1,1,2,2-$C_2D_2Cl_4$ was added to the sample, and then a Teflon plug is inserted so that the bottom is just above the sample, creating a slight free volume above the sample. The samples were stored for 1 day before the measurements were performed. In this case, 1,1,2,2-$C_2D_2Cl_4$ was the solvent of preference due to its high boiling point, which permitted NMR experiments at elevated temperatures.

**F. Network Structure Analysis by Dynamic Mechanical Experiments.** The mean molar mass of network chains was calculated from the slope of the linear part of the dependence of the modulus at temperatures above $T_g$. The following equation relates the slope of the dependence ($E'/T$) to the molar mass of network chains between *c*hemical cross-links and chain *e*ntanglements, $M_{c+e}$, in kg/kmol:[45,46]

$$M_{c+e} = 3\rho RT(1 - x)/E' \qquad (1)$$

where $\rho$ is the specific density in kg/m$^3$, $R$ is the gas constant that equals 8.3 J/(mol K), $E'$ is the modulus in Pa, and $x$ is the volume fraction of 2-ethylhexyl fragments of EHA. Suggesting density additivity, a value of $x$ was calculated from the specific density of network chains (PEGDA) and alkylic fragment of EHA 1.11 and 0.86 g/cm$^3$, respectively. Equation 1 is applicable to affine networks of the same chain length and without network defects. It is recognized that the effective number of elastically active network chains reduces in networks with spatial clustering of cross-links.[5−7] This means that a value of $M_{c+e}$ is overestimated with eq 1 in the case of heterogeneous networks.

**G. Network Structure Analysis by $^1$H NMR $T_2$ Relaxation.** At temperatures about 100−150 K above $T_g$, the $T_2$ relaxation time for elastomer networks is very sensitive to the conformational mean position of network chains, which is affected by the presence of chemical and physical network junctions. At these temperatures, $T_2$ for cross-linked elastomers is nearly independent of temperature. The temperature independence of $T_2$ at temperatures well above $T_g$ is attributed to constraints, which limit the number of possible conformations of a network chain with respect to those of a free chain. In other words, due to the high segmental mobility, the network chains take a mean conformational position, which

depends on the number of statistical segments between network junctions.

The $T_2$ value at this high-temperature plateau, $T_2^p$, has been quantitatively related to the number of statistical segments in network chains.[47,48] For a Gaussian chain, in which the average squared distance between network junctions is much shorter than the contour chain length, the $T_2^p$ value is related to $Z$ statistical segments between the network junctions:[47,48]

$$Z = T_2^p/(aT_2^{rl}) \quad (2)$$

where $a$ is the theory coefficient, which depends on the angle between the segment axis and the internuclear vector for the nearest nuclear spins at the main chain. For polymers containing aliphatic protons in the main chain, the coefficient $a$ is close to $6.2 \pm 0.7$.[48] The $T_2^{rl}$ value, which is measured for swollen samples below $T_g$, is related to the strength of intrachain proton−proton interactions in the rigid lattice. The $T_2^{rl}$ value for 1,1,2,2-$C_2D_2Cl_4$ swollen compounds PEGDA (100)−PEGDA/EHA(10:90) varies from 7.7 to 9.3 $\mu$s at −166 °C. Using the number of backbone bonds in the statistical segment, $C_\infty$, the molar mass of network chains between chemical and physical network junctions, $M_{c+e}$ is calculated:

$$M_{c+e} = ZC_\infty M_u/n \quad (3)$$

where $M_u$ is the molar mass per elementary chain unit for the polymer chain and $n$ is the number of backbone bonds in an elementary chain unit. According to different authors, $C_\infty$ for poly(ethylene oxide) (PEO) varies from 3.8 to 6.9 main chain bonds.[49−51] The mean value of 5.0 is taken for the calculation. It is assumed that the relative contribution of a network chain to the total relaxation function for heterogeneous networks is proportional to the number of protons attached to this chain. Accordingly, the mean molar mass of network chains, as measured by the NMR method, should be related to the weight-averaged molar mass of network chains. The network density in the networks studied is largely determined by the density of chemical cross-links, since the length of the PEO chain of PEGDA is significantly shorter compared to the mean molar mass between apparent chain entanglements in PEO (700 and about 2000 g/mol,[49−51] respectively). The maximum, relative error of this NMR network density determination is largely determined by uncertainty in $C_\infty$ for PEO, which is about 35%.

## Results

**Glass Transition.** As expected, the glass transition temperature of the compounds increases linearly upon an increase in the content of difunctional monomer, as shown in Figure 2. Fox and Loshaek or similar equations can describe the dependence[52]

$$T_g = T_g^\infty + k_n/M_c \quad (4)$$

where $T_g^\infty$ is the $T_g$ of a polymer of infinite molecular weight and $k_n$ is a material constant. It is mentioned that this equation does not take into account the "copolymer effect" of network junctions, high functionality of network junctions, non-Gaussian chain statistics, and the effect of dangling chains.[53−57]

The temperature dependence of modulus is shown in Figure 3. A rubber-elastic plateau is observed above −20 °C, but slippage of samples out of clamps causes sharp decrease in $E'$ above 50 °C for samples with high EHA content. Both $T_g$ and $E'$ decrease upon increasing EHA content that corresponds to a decrease in the cross-link density. The slope of the dependence of $E'$ on temperature in the plateau range is used for the calculation of molar mass of network chains. Obtained values will be compared below with those determined by the $^1$H $T_2$ experiment.

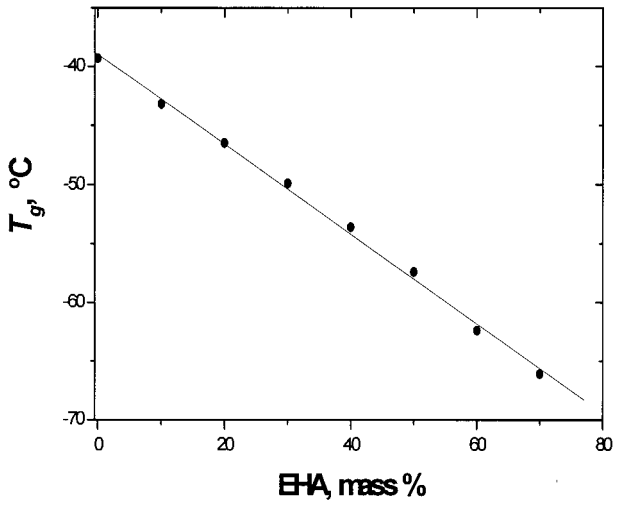


**Figure 2.** $T_g$ of cured acrylates against the content of EHA. The line represents the result of a linear regression analysis: intercept = −39.0 ± 0.4 °C; slope = −0.381 ± 0.009 °C (mass %)$^{-1}$. The correlation coefficient equals 0.998.

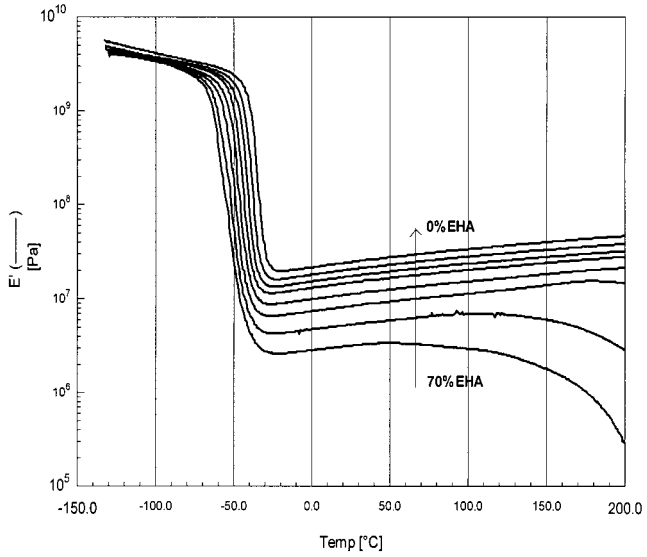


**Figure 3.** Temperature dependence of storage modulus, $E'$, of cured acrylates with increasing amounts of EHA.

**Network Structure by $^1$H NMR $T_2$ Relaxation.** The relaxation rate, $1/T_2$, at 50 °C for samples as a whole reveals also a linear dependence against the content of monofunctional monomer (see Figure 4). Since the relaxation rate at temperatures well above $T_g$ is proportional to the network density,[34,47,48] it can be concluded from results in Figure 4 that the cross-link density in cured acrylates is proportional to the content of difunctional monomer.

To obtain more detailed information on network structure in the compounds, the $T_2$ relaxation experiment is performed on partially swollen in 1,1,2,2-$C_2D_2Cl_4$ networks. The $T_2$ decay for compounds PEGDA-(100)−PEGDA/EHA(20:80) as a whole and swollen samples consists of fast and slowly decaying components with characteristic decay time $T_2^s$ and $T_2^l$, respectively. The superscripts "s" and "l" relate to short ($T_2^s$) and long ($T_2^l$) relaxation time, respectively. The relative fraction of these components (%$T_2^s$ and %$T_2^l$) corresponds to the content of hydrogen in materials, which are responsible

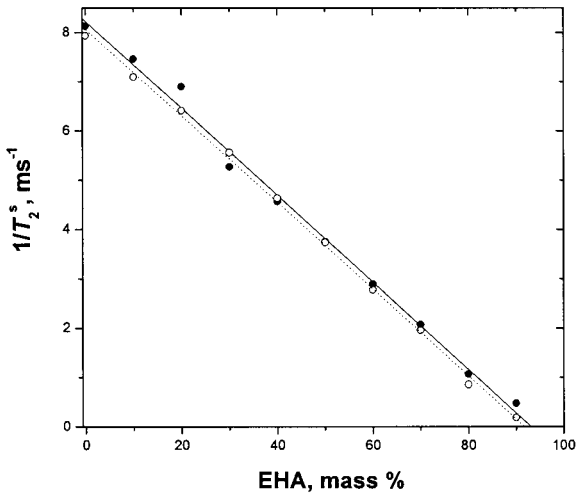


**Figure 4.** $T_2$ relaxation rate at 50 °C against the content of EHA for cured acrylates as a whole (closed circles) and swollen samples (open circles). The relaxation rate for swollen samples corresponds to its value at maximum of dependence $(T_2^s)^{-1}$ against solvent content (see Figure 7). The solid line represents the result of a linear regression analysis for samples as a whole: intercept = 8.2 ± 0.2 ms$^{-1}$; slope = −0.088 ± 0.003 ms$^{-1}$(mass %)$^{-1}$; the correlation coefficient equals 0.997. The dotted line represents the result of a linear regression analysis for swollen samples: intercept = 8.07 ± 0.07 ms$^{-1}$; slope = −0.088 ± 0.001 ms$^{-1}$ (mass %)$^{-1}$; the correlation coefficient equals 0.9992.

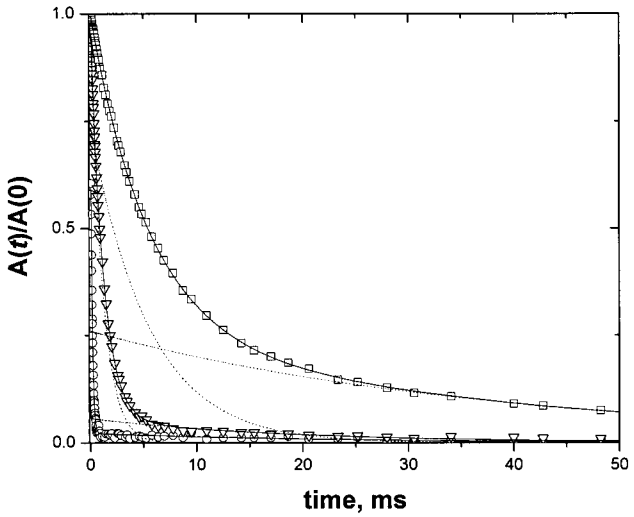


**Figure 5.** $T_2$ decay for cured acrylates with different content of EHA: PEGDA/EHA(90:10), circles; PEGDA/EHA(20:80), down triangles; PEGDA/EHA(10:90), squares. The sold line represents the result of a least-squares adjustment of the decay with a linear combination of two exponential functions. Dotted lines show separate components for PEGDA/EHA(20:80) and PEGDA/EHA(10:90). The samples were swollen in 1,1,2,2-$C_2D_2Cl_4$ (46 vol %). The measurements were performed at 50 °C. Only the initial part of the decay is shown for compound PEGDA/EHA(10:90).

for these relaxations. $\%T_2^s$ and $\%T_2^l$ for cured PEGDA(100)−PEGDA/EHA(20:80) equals about 96−99.5% and 4−0.5%, respectively (see Figure 5). The major component reveals $T_2$ relaxation time, which is typical for cross-linked rubbers, i.e., in the range of milliseconds or shorter. A small fraction of compounds PEGDA(100)−PEGDA/EHA(20:80) shows high molecular mobility. This fraction presumably originates from residual uncured material and low molar mass photoinitiator. Thus, the amount of network defects is small in cured PEGDA(100)−PEGDA/EHA(20:80). Cured PEGDA/EHA(10:90)

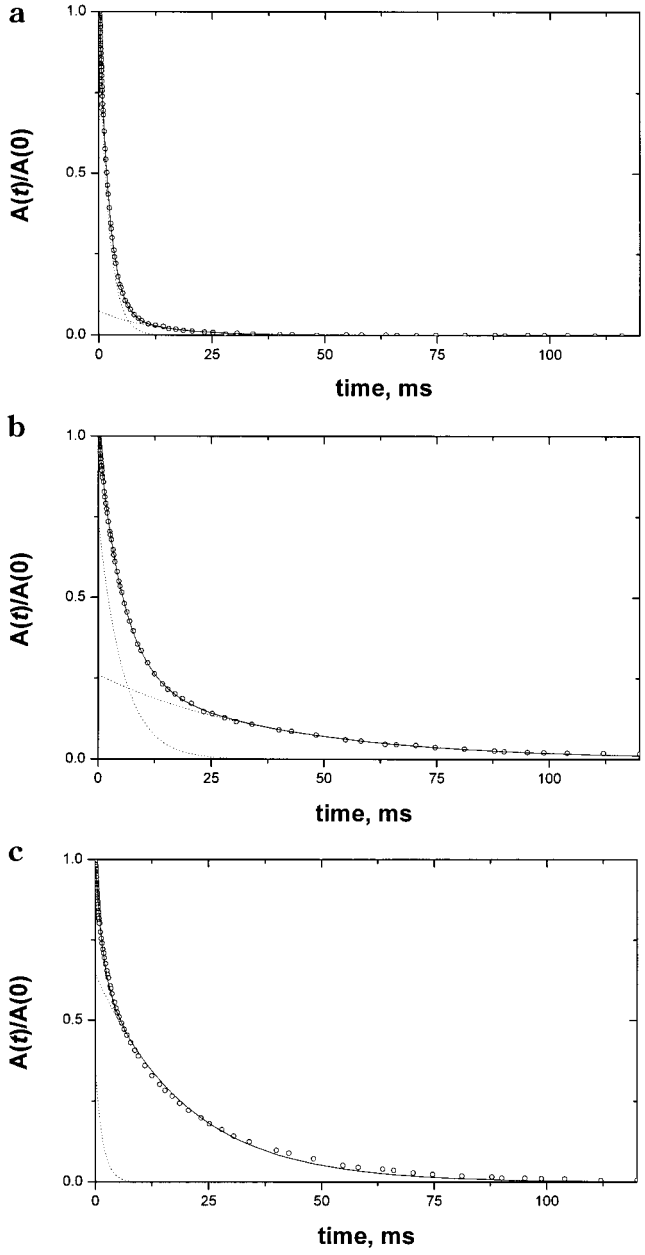


**Figure 6.** $T_2$ decay for cured compound PEGDA/EHA(10:90) without solvent (a) and with 46 vol % (b) and 90 vol % (c) of 1,1,2,2-$C_2D_2Cl_4$. The solid line represents the result of a least-squares adjustment of the decay with a linear combination of two exponential functions. Dotted lines show separate components.

has a significantly larger fraction of slowly decaying component (see Figures 5 and 6). The relaxation time $T_2^l$ for this sample is in the range that is typical for highly mobile oligomer molecules, long dangling chain ends, chain loops, and loosely cross-linked chains.[39−41] This relaxation is assigned to the relaxation of network defects in compound PEGDA/EHA(10:90).

The dependence of $T_2^s$ on the solvent content in PEGDA/EHA(10:90) is similar to those for networks with a large fraction of temporary chain entanglements and network defects.[34,38] Starting from a low solvent content, $V_s$, $T_2^s$ increases (see Figures 7−9), which can be the result of the following phenomena: (i) the disentanglement of the network chains, (ii) an increase in the frequency of the large spatial scale chain motion, and (iii) a slight decrease in the strength of the interchain proton dipole−dipole interactions. At $V_s \approx 0.5$, $T_2^s$

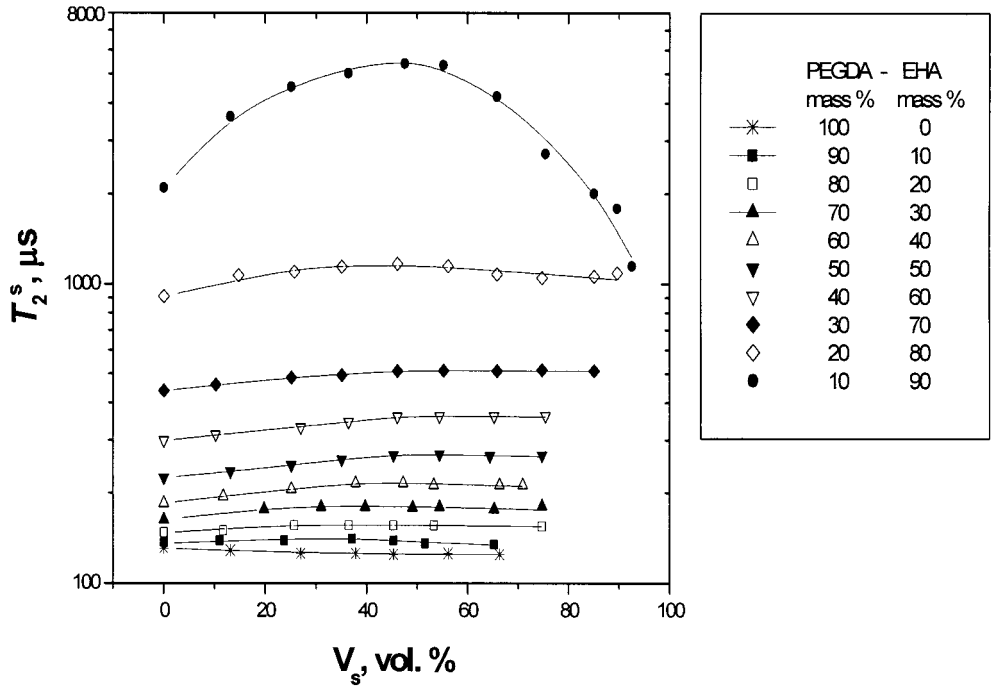


**Figure 7.** $T_2^s$ relaxation rate at 50 °C for cured acrylates against volume fraction of 1,1,2,2-$C_2D_2Cl_4$ in swollen networks. The content of PEGDA and EHA is shown on the inset.

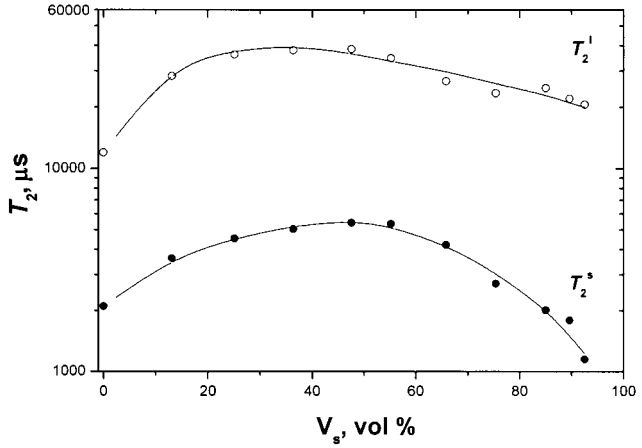


**Figure 8.** Relaxation time $T_2^s$ and $T_2^l$ at 50 °C for PEGDA/EHA(10:90) against the volume fraction of 1,1,2,2-$C_2D_2Cl_4$ in the swollen sample.

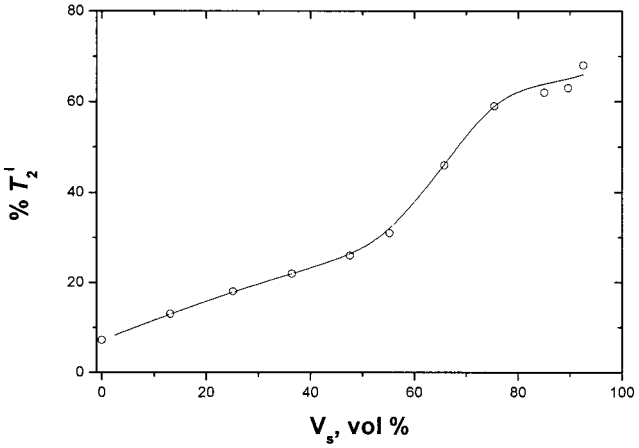


**Figure 9.** Relative fraction of $T_2^l$ relaxation component at 50 °C for PEGDA/EHA(10:90) against the volume fraction of 1,1,2,2-$C_2D_2Cl_4$ in the swollen sample.

reaches a maximum value. At higher values of $V_s$, $T_2^s$ decreases until the state of equilibrium swelling is reached. This decrease in $T_2^s$ is thought to reflect the increase in the intrachain, proton dipole−dipole interactions as a result of the network chain elongation upon a progressive increase in the solvent fraction in swollen gels.[58] An increase in $\%T_2^l$ with increasing of solvent content is apparently caused by chain disentanglement which causes a distinct difference in mobility of partially strained network chains and highly mobile disentangled network defects (see Figure 9).

The dependence of $T_2^s$ on the content of solvent in swollen compounds is compared for all samples in Figure 7. $T_2^s$ of compounds PEGDA(100)−PEGDA/EHA-(30:70) is hardly affected by swelling. This suggests that the amount of temporary chain entanglements and network defects is low in these samples. Therefore, the mean length of polymer chains between chemical crosslinks in PEGDA(100)−EGDA/EHA(30:70) should be comparable to or smaller than $M_e$, which is about 2000 g/mol for PEO.[49−51] The maximum of the dependence of $T_2$ on $V_s$ is observed for all samples at $V_s$ of about 50%. The relaxation rate at the maximum, $1/(T_2^s)^{max}$, is compared for the complete series of samples in Figure 4. A fairly good correlation of $1/(T_2^s)^{max}$ with the storage modulus gives an additional proof that the NMR characteristic is directly related to the network structure (see Figure 10).

The mean molar mass of network chains is calculated from $(T_2^s)^{max}$.[59] The obtained values are compared with those from the mechanical experiment in Figure 11. The results of these two methods are in rather good agreement, if one accounts for assumptions made for the calculation of the $M_{c+e}$ from the NMR and mechanical data and large uncertainty in $C_\infty$ for PEO. The crosslink density in cured acrylates decreases with increasing the content of monofunctional monomer. The molar mass of network chains is significantly smaller compared to the molar mass of difunctional monomer for cured acrylates containing more than 20 wt % of

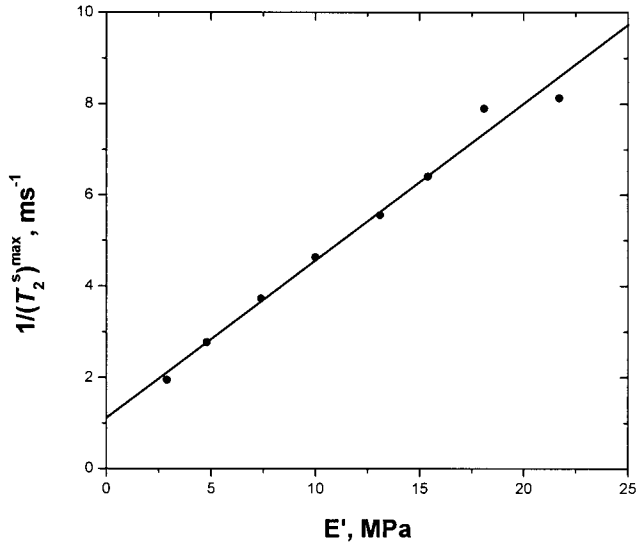


**Figure 10.** Relaxation rate $(1/T_2^s)^{max}$ for samples partially swollen in 1,1,2,2-$C_2D_2Cl_4$ against the storage modulus at 0 °C. The rubbery plateau is observed for all samples at this temperature. The line represents the result of a linear regression analysis: intercept = $1.1 \pm 0.3$ $ms^{-1}$; slope = $0.34 \pm 0.02$ $ms^{-1}$ $(MPa)^{-1}$. The correlation coefficient equals 0.992.

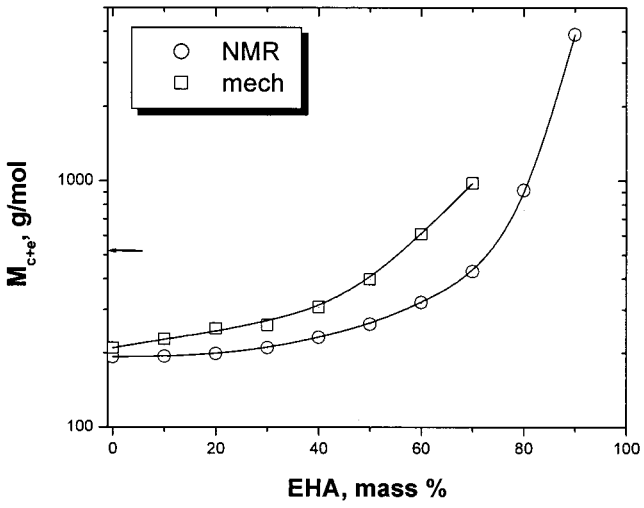


**Figure 11.** Mean molar mass between chemical cross-links and trapped chain entanglements in cured PEGDA/EHA against EHA content. $M_{c+e}$ is determined by the NMR $T_2$ relaxation method[47,48] and from the slope of the dependence of plateau modulus on temperature using eq 1. The molar mass of PEGDA is shown by arrow.

PEGDA. A possible explanation of this result will be given below.

**Chemistry of Curing As Studied by $^{13}C$ NMR Spectroscopy.** To ensure that all cross-links are mainly generated from acrylate polymerization, the $^{13}C$ NMR spectra are recorded for uncured and cured PEGDA-(100). Curing causes the following changes in the $^{13}C$ NMR MAS spectrum (see Figure 12):

(i) All resonances in the cured compound are significantly broader compared to those of the initial compound (see Figure 12a,b), which is apparently caused by a restriction of chain mobility due to curing.

(ii) Resonances at 128−136 ppm, which originate from carbon atoms of the double bond, are hardly detected after curing, indicating high conversion of double bonds. This is in the agreement with the results of FT-IR that show more than 96% conversion.

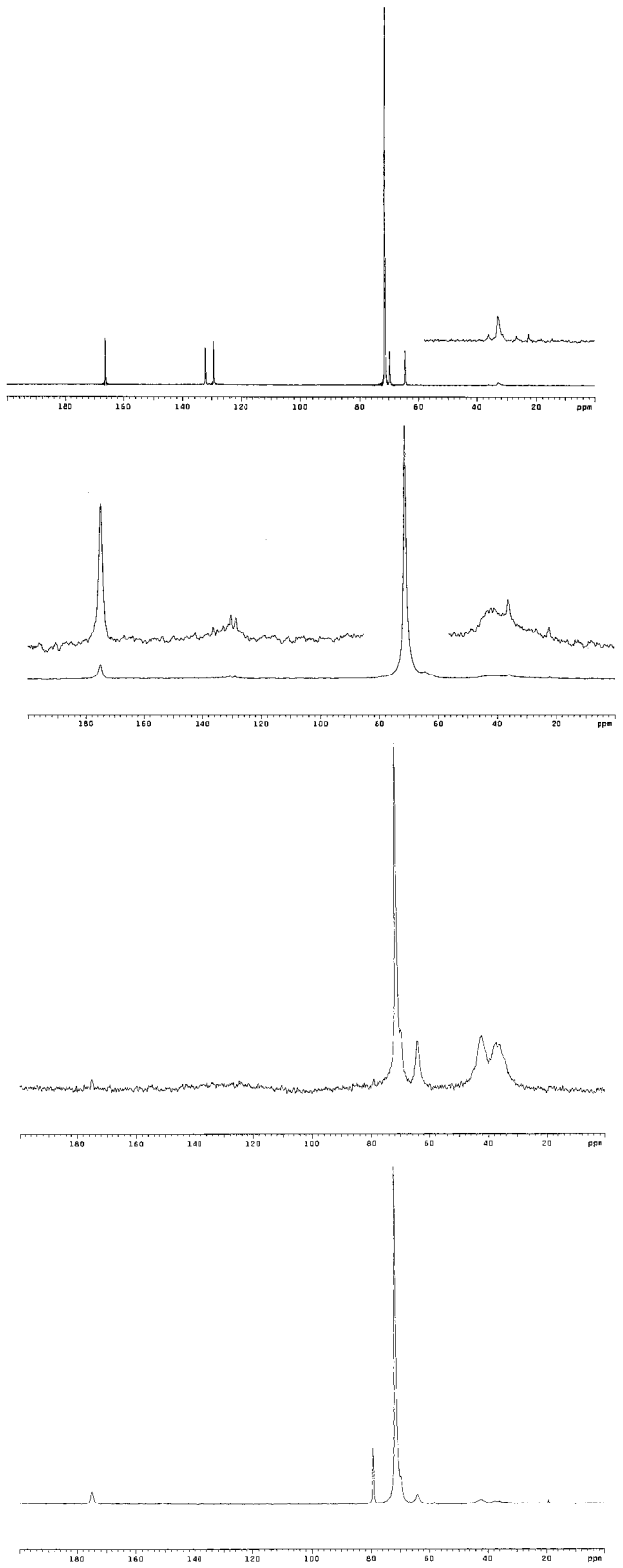


**Figure 12.** $^{13}C$ MAS spectrum for uncured (a) and cured (b) PEGDA(100) and $^{13}C$ CP/MAS spectra for the cured compound recorded at $\tau_{cp}$ of 0.025 ms (c) and 20 ms (d). To enhance the spectral resolution of $^{13}C$ CP/MAS spectra, about 30 mass % of $CHCl_3$ was added to the cured compound. The resonances are assigned to the following carbon atoms in initial mixture: 71.3 ppm, $OCH_2$ carbons in the middle part of PEGDA; 64.5 and 69.7 ppm, $OCH_2$ carbons in $\alpha$ and $\beta$ positions to carbonyl carbon atom at chain ends, respectively; 132.0 and 129.3 ppm, $CH_2$ and CH carbons of vinyl group, respectively; 166.4 ppm, carbonyl carbon. The spectra amplitude is adjusted to the peak at 71.3 ppm.

(iii) The resonance for carbonyl carbon shifts from 166.4 to 174.9 ppm upon curing. This change in the chemical shift is caused by the loss of conjugation due to double-bond opening. A lack of the resonance at 166.4 ppm for the cured compounds provides additional proof of the high conversion of double bonds.

(iv) Broad resonances that are centered at 37 and 42 ppm appear in the spectrum of the cured compound. These resonances correspond to methylene ($CH_2$) and methane (CH) carbons of aliphatic chains, which is formed by acrylate curing.

The resonances at 37 and 42 ppm can originate from cross-links and products of side reactions. To prove that these resonances originate from cross-links, $^{13}C$ NMR CP/MAS spectra are recorded. The $^{13}C$ resonances of highly immobilized phases/components in complex materials are enhanced in $^{13}C$ CP/MAS spectra at short cross-polarization time ($\tau_{cp}$) and diminish at very long $\tau_{cp}$. At the opposite, the resonances from mobile phases/components are enhanced at long $\tau_{cp}$ and are hardly detected at very short $\tau_{cp}$. It should be mentioned that the line intensity as a function of $\tau_{cp}$ in $^{13}C$ CP/MAS spectra is also affected by the chemical origin of carbon atoms. In the case of similar molecular mobility, the buildup of the magnetization upon increasing $\tau_{cp}$ is faster for carbon atoms of methylene, methane, and methyl groups when compared to carbonyl and quaternary carbon atoms. It can be seen from Figure 12c,d that broad resonances at 36−42 ppm are enhanced at short $\tau_{cp}$. These resonances vanish at long $\tau_{cp}$. It is noted that the carbonyl resonance is not observed in the spectrum at short $\tau_{cp}$ because of low cross-polarization efficiency. Since motions of network junctions are strongly hindered compared to that of network chains, the $^{13}C$ CP/MAS spectra provide strong evidence that the resonances at 36−42 ppm originate from carbon atoms from cross-link junctions. Moreover, this assignment is confirmed by means of $^{13}C$ NMR MAS spectra of a saponification product of a typical UV-cured polyacrylate. Saponification allows isolating cross-link junctions fragments from polyether chains. The $^{13}C$ NMR spectrum of the saponification product is similar to that of poly(sodium acrylate). The spectrum contains resonances at about 40, 46, and 185 ppm that correspond to methylene, methine, and carbonyl carbon atoms, respectively. The integral intensity of the broad resonances at 36−42 ppm for cured PEGDA(100) is about 2 times larger when compared to that of carbonyl carbon atoms (Figure 12b), which should be observed for acrylic polymerization, if no side reactions occur.

Thus, in examining networks by $^{13}C$ NMR, we observe that the conversion is high, and the contribution or effect of side reactions that generate extra cross-links is negligible.

## Discussion

On the basis of NMR and mechanical data, an idealized structure for networks PEGDA(100) and PEGDA/EHA(80:20) is proposed in Figure 13. Spatial distribution of network junctions is heterogeneous in these networks, which causes uncertainty in the calculation of the total number of network junctions per unit volume from the modulus of the material. Well-established theories of the rubber elasticity are derived for perfect networks with nearly identical length of network chains and homogeneous distribution of network junctions.[2,3]

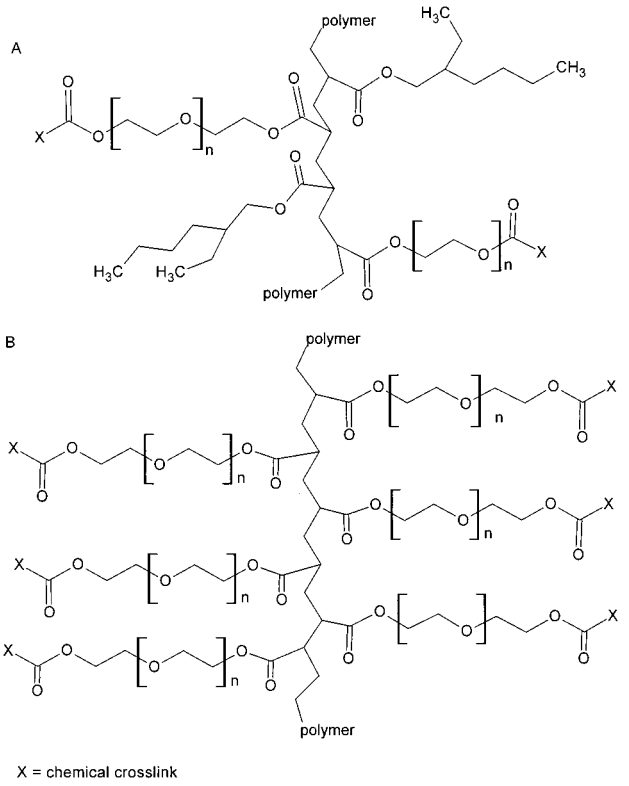


**Figure 13.** Suggested network structure for compounds PEGDA/EHA(80:20) (A) and PEGDA(100) (B).

These theories suggest that network chains obey Gaussian chain statistics, which requires at least 50 rotatable main-chain bonds. It is recognized that the network topology is crucial in rubber elasticity[4−7,60] and "that global properties are not very suitable to quantify these (heterogeneity) effects. Most importantly, heterogeneity effects can hardly be determined by quasi-static mechanical measurements such as stress−strain experiments. Local methods (which probe molecular properties) are well suitable for the determination of heterogeneity effect".[7] Thus, classical theories cannot be used in our case for the calculation of the mean molar mass of network chains from the modulus, and vice versa. Qualitatively, the modulus in strongly heterogeneous networks is lower compared to its value predicted by classical rubber elasticity theories, since the number of elastically active cross-links is reduced due to heterogeneity.[4,6] Long chains and loosely cross-linked domains determine in large extent the low deformation modulus. Network heterogeneity improves significantly ultimate strength and elongation at break, since network heterogeneity allows for more effective distribution of stress throughout the material due to relaxation of softer areas.[2,61]

At present, no accepted approach is available that allows one to relate the modulus to the molar mass of network chains attached to ziplike network junctions. To relate the modulus to the network structure, it will be necessary to determine first what is the average length of the polyacrylic chain bearing network junctions and then to perform experiments to demonstrate how these chains respond to applied stress. Then one can comment on whether these polyacrylic chains make a significant contribution to the modulus relative to the polyether chains.

## Conclusions

The network structure in UV-cured acrylates is studied with proton NMR relaxation, $^{13}C$ NMR spectroscopy, and mechanical experiments. The following conclusions are made from this study: (1) the NMR $T_2$ relaxation method shows good correlation with mechanical tests to determine molar mass between cross-links. (2) The cured compounds contain a small fraction of residual monomers. Examining networks by $^{13}C$ NMR spectroscopy, we observe that the conversion is high, and the contribution or effect of side reactions that generate extra cross-links is negligible. (3) It is also possible with the $T_2$ relaxation method to estimate the amount of highly mobile chains, i.e., extractable materials and network defects chemically attached to network chains, i.e., dangling chains and chain loops. (4) An increase in the content of monofunctional monomer causes a significant decrease in the cross-link density because the monofunctional monomer acts as a chain extender. A large fraction of monofunctional monomer (above 80 mass %) causes significant fraction of network defects.

**Acknowledgment.** The authors are thankful to G. Heinrich, J. E. Mark, D. Göritz, and J. P. Cohen-Addad for stimulating discussions during a minisymposium on heterogeneous polymer networks held at DSM Research.

## References and Notes

(1) Rabek, J. F. In *Radiation Curing in Polymer Science and Technology. Fundamentals and Methods;* Fouassier, J. P., Rabek, J. F., Eds.; Elsevier Applied Science: London, 1993; Vol. 1, p 329.
(2) Mark, J. E.; Erman, B. *Rubberlike Elasticity. A Molecular Primer*; Wiley: New York, 1988.
(3) Heinrich, G.; Straube, E.; Helmis, G. *Adv. Polym. Sci.* **1988**, *85*, 33.
(4) Vilgis, T. A.; Heinrich, G. *Angew. Makromol. Chem.* **1992**, *202/203*, 243.
(5) Vilgis, T. A.; Heinrich, G. *Kautsch. Gummi Kunstst.* **1992**, *45*, 1006.
(6) Schimmel, K.-H.; Heinrich, G. *Colloid Polym. Sci.* **1991**, *269*, 1003.
(7) Vilgis, T. A.; Heinrich, G. *Makromol. Theory Simul.* **1994**, *3*, 271.
(8) Dias, A. A.; Hartwig, H.; Jansen, J. F. G. A. *Surf. Coat. Int.* **2000**, *83*, 382.
(9) Bauer, D. R. *Prog. Org. Coat.* **1986**, *14*, 45.
(10) Koenig, J. L. *J. Appl. Polym. Sci.* **1998**, *70*, 1359 and references therein.
(11) Gronski, W.; Hoffman, U.; Simon, G.; Wutzler, A.; Straube, E. *Rubber Chem. Technol.* **1992**, *65*, 63.
(12) McBrierty, V. J.; Packer, K. J. *Nuclear Magnetic Resonance in Solid Polymers*; Cambridge University Press: Cambridge, 1993.
(13) Schmidt-Rohr, K.; Spiess, H. W. *Multidimensional Solid-State NMR and Polymers*; Academic Press: London, 1994.
(14) Callaghan, P. T. *Principles of Nuclear Magnetic Resonance Microscopy;* Clarendon Press: Oxford, 1991.
(15) Blümler, P.; Blümich, B. In *NMR Basic Principles and Progress;* Diehl, P., Fluck, E., Günther, H., Kosfeld, R., Seelig, J., Eds.; Springer-Verlag: Berlin, 1994; Vol. 30.
(16) Adriaensens, P.; Pollaris, A.; Vanderzande, D.; Gelan, J.; White, J.; Dias, A. J.; Kelchtermans, M. *Macromolecules* **1999**, *32*, 4692.
(17) McCall, D. W. *Acc. Chem. Res.* **1971**, *4*, 223.
(18) Schaefer, J.; Stejskal, E. O.; Buchdahl, R. *Macromolecules* **1977**, *10*, 384.
(19) Parker, A. A.; Marcinko, J. J.; Rinaldi, P.; Hedrick, D. P.; Ritchey, W. M. *J. Appl. Polym. Sci.* **1993**, *48*, 677.
(20) Simon, G. P.; Allen, P. E. M.; Bennett, D. J.; Williams, D. R. G.; Williams, E. H. *Macromolecules* **1989**, *22*, 3555.
(21) Allen, P. E. M.; Bennet, D. J.; Hagias, S.; Hounslow, A. M.; Ross, G.; Simon, G. P.; Williams, D. R. G.; Williams, E. H. *Eur. Polym. J.* **1989**, *25*, 785.
(22) Dietz, J. E.; Cowans, B. A.; Scott R. A.; Peppas, N. A. *ACS Symp. Ser.* **1997**, *673*, 28.
(23) Heatley, F.; Ali, M.; Godward, J.; Stonebank, K.; Wattas, D. C.; Devlin, H. *Polymer* **1997**, *38*, 2041.
(24) Lungu, A.; Neckers, D. C. *Macromolecules* **1995**, *28*, 8147.
(25) Jager, W. F.; Lungu, A.; Chen, D. Y.; Neckers, D. C. *Macromolecules* **1997**, *30*, 780.
(26) Scott, R.; Cowans, B. A.; Peppas, N. A. *J. Polym. Sci., Part B: Polym. Phys.* **1999**, *37*, 1953.
(27) Moore, J. E. In *Chemistry and Properties of Crosslinked Polymers*; Labana, S. S., Ed.; Academic Press: New York, 1977; p 535.
(28) Martin, S. J.; McBrierty, V. J.; Dowling, J.; Douglass, D. C. *Macromol. Rapid Commun.* **1999**, *20*, 95.
(29) Andfreis, M.; Koenig, J. L. *Adv. Polym. Sci.* **1989**, *89*, 69.
(30) Kinsey, R. A. *Rubber Chem. Technol.* **1990**, *63*, 407.
(31) Cohen-Addad, J. P. *Prog. NMR Spectrosc.* **1993**, *25*, 1.
(32) Whittaker, A. K. In *Annual Report on NMR Spectroscopy*; Web, G. A., Ando, I., Eds.; Academic Press: San Diego, 1997; Vol. 34, p 105.
(33) Cohen-Addad, J. P.; Pellicioli, L.; Nusselder, J. J. *Polym. Gels Networks* **1997**, *5*, 201.
(34) Litvinov, V. M.; Barendswaard, W.; van Duin, M. *Rubber Chem. Technol.* **1998**, *71*, 105.
(35) Charlesby, A. In *Radiation effects on Polymers;* Clough, R. L., Shalaby, S. W., Eds.; ACS Symposium Series; American Chemical Society: Washington, DC, 1991; Vol. 475, p 193 and references therein.
(36) Cohen-Addad, J. P.; Girard, O. *Macromolecules* **1992**, *25*, 593.
(37) Litvinov, V. M. *Int. Polym. Sci. Technol.* **1988**, *15*, T/28.
(38) Litvinov, V. M.; Steeman, P. A. M. *Macromolecules* **1999**, *32*, 8476.
(39) Weber, H. W.; Kimmich, R. *Macromolecules* **1993**, *26*, 2597.
(40) Kimmich, R.; Köpf, M.; Callaghan, P. *J. Polym. Sci., Part B: Polym. Phys.* **1991**, *29*, 1025.
(41) Kulagina, T. P.; Litvinov, V. M.; Summanen, K. T. *J. Polym. Sci., Part B: Polym. Phys.* **1993**, *31*, 241.
(42) Sandakov, G. I.; Tarasov, V. P.; Volkova, N. N.; Ol'khov, Y. A.; Smirnov, L. P.; Erofeev, L. N.; Khitrin, A. K. *Vysokomol. Soedin., Ser. B* **1989**, *31*, 821.
(43) Volkova, N. N.; Sandakov, G. I.; Sosikov, A. I.; Ol'khov, Y. A.; Smirnov, L. P.; Summanen, K. T. *Polym. Sci. USSR* **1992**, *34*, 127.
(44) Decker, C.; Moussa, K. *Makromol. Chem.* **1988**, *189*, 2381.
(45) Flory, P. J. *Principles of Polymer Chemistry*; Cornell University Press: Ithaca, NY, 1953.
(46) Treloar, L. R. G. *The Physics of Rubber Elasticity*, 3rd ed.; Clarendon Press: Oxford, 1975.
(47) Gotlib, Yu. Ya.; Lifshits, M. I.; Shevelev, V. A.; Lishanskii, I. A.; Balanina, I. V. *Polym. Sci. USSR* **1976**, *18*, 2630.
(48) Fry C. G.; Lind, A. C. *Macromolecules* **1988**, *21*, 1292.
(49) Graessley, W. W. *Polymer* **1981**, *22*, 1329.
(50) Aharoni, S. M. *Macromolecules* **1983**, *16*, 1722.
(51) Wu, S. *Polym. Eng. Sci.* **1992**, *32*, 823.
(52) Fox, T. G.; Loshaek, S. *J. Polym. Sci.* **1955**, *15*, 371.
(53) Andrady, A. L.; Sefcik, M. D. *J. Polym. Sci., Polym. Phys. Ed.* **1983**, *21*, 2453.
(54) Stutz, H.; Illers, K.-H.; Mertes, J. *J. Polym. Sci., Part B: Polym. Phys. Ed.* **1990**, *28*, 1483.
(55) Hale, A.: Macosko, C. W.; Bair, H. E. *Macromolecules* **1991**, *24*, 2610.
(56) Shefer, A.; Gottlieb, M. *Macromolecules* **1992**, *25*, 4036.
(57) Reekmans, B. J.; Shi, J.-F.; Pyati, M.; MacKnight, W. J.; Lillya, C. P. *Acta Polym.* **1995**, *46*, 12.
(58) Schmidt, C.; Cohen-Addad, J. P. *Macromolecules* **1989**, *22*, 142.
(59) The quantitative determination of the network density in compounds can be complicated due to the presence of short chain branches that originate from monofunctional monomer. It is known that the mobility of short side groups and chain-end blocks is somewhat higher compared to the mains chain, and it increases when moving toward the chain end.[39−41] In a highly simplified approach, $1/(T_2^s)^{max}$ is a weight average of the relaxation of the backbone protons of network chains ($1/T_2^{net}$) and those of the side chains ($1/T_2^{sc}$) which originate from the monofunctional monomer: $1/(T_2^s)^{max} = f_n(1/T_2^{net}) + (1 - f_n)(1/T_2^{sc})$, where $f_n$ is the fraction of backbone protons. It is noted that $T_2^{net}$ and $T_2^{sc}$ could be determined using selective proton relaxation experiments with high-resolution NMR spectroscopy. According to a least-squares fit analysis of simulated decays, the decay can be decomposed on two components, if $T_2$ values differ by more than a factor of 2−3. Since the $T_2$ relaxation of compounds PEGDA(100)−PEGDA/

EHA(20:80) is described by a single-exponential function, it suggests that the mobility of side chains is strongly coupled to that of network chains, which results in similar values for $T_2^{net}$ and $T_2^{sc}$. $T_2^{net}$ is calculated from $1/(T_2^s)^{max}$, suggesting that $T_2^{sc} = 2T_2^{net}$.

(60) Sharaf, M. A.; Mark, J. E.; Al Hosani, Z. Y. *Eur. Polym. J.* **1993**, *29*, 809.

(61) Mark, J. E. *Acc. Chem. Res.* **1985**, *18*, 202.

MA010066U